

# Bond Softening Indices Studied by the Fragility Spectra for Proton Migration in Formamide and Related Structures

Published as part of *The Journal of Physical Chemistry virtual special issue "Paul Geerlings Festschrift"*.

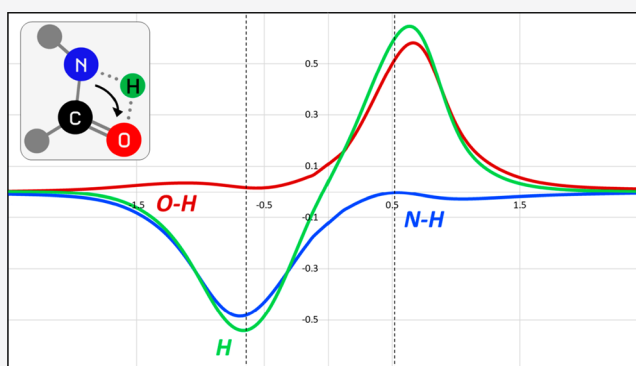
Piotr Ordon,<sup>\*,†</sup> Jarosław Zaklika,<sup>‡</sup> Mateusz Jędrzejewski,<sup>‡</sup> and Ludwik Komorowski<sup>‡</sup>

<sup>†</sup>Department of Physics and Biophysics, Wrocław University of Environmental and Life Sciences, ul. Norwida 25, 50-373 Wrocław, Poland

<sup>‡</sup>Department of Physical and Quantum Chemistry, Wrocław University of Science and Technology, Wyb. Wyspiańskiego 27, 50-370 Wrocław, Poland

## Supporting Information

**ABSTRACT:** Computational scheme to obtain bond softening index  $\lambda$ , defined within the conceptual DFT, has been obtained with the use of the reaction fragility (RF) concept. Numerical results were obtained with the RF spectra for the proton transfer reaction in formamide molecule ( $\text{H}_2\text{NCHO}$ ) and the water assisted proton migration in  $\text{H}_2\text{NCHO}\cdot\text{H}_2\text{O}$  complex. Double proton transfer reaction in the formamide dimer,  $(\text{H}_2\text{NCHO})_2$ , and its analogues,  $(\text{H}_2\text{NCHS})_2$  and  $(\text{H}_2\text{NCHO})\cdot(\text{H}_2\text{NCHS})$ , have also been studied. The atomic and bond RF spectra clearly describe the density reorganization in the backbone of each molecule, resulting from proton displacement in the systems. The obtained softening indices have been calculated for hydrogen atoms in the reactant state (RS) and product state (PS) configuration. These indices provide fine characteristics for the local sensitivity of the reacting system to a disturbance of the position of a chosen atom.



## 1. INTRODUCTION

Quantum theory does not provide any direct definition of the chemical bond. The molecule is formed due to an equilibrium between electrostatic repulsive forces of the nuclei glued by the attractive interactions to the electron density. Once the positions of nuclei get reorganized during some chemical reaction, another equilibrium structure is obtained with another pattern of electron density that holds this structure together. However, for practical reasons, chemists demand the mechanism of the reaction. The mechanism is basically the sequence of the bond formation and cleavage for all the atoms involved in a chemical reaction and the tracking of deformation of the original structure into the new atomic positions. This mechanism description represents the very essence of the chemical knowledge, both on the experimental and on the theoretical level. The firm ground for the description of the geometrical transformation and atomic trajectories into the new positions has been created by Fukui<sup>1</sup> as the intrinsic reaction coordinate (IRC) formalism, followed by the reaction path Hamiltonian introduced by Miller et al.<sup>2,3</sup> The role of complexity of an actual process has been focused on by Klipenstein et al.,<sup>4</sup> and the modern chemical dynamic simulations have been presented by Hase et al.<sup>5</sup> However, the existence of bonds and their modifications is fundamental in practical chemistry. It is supported by the quantum chemical

picture of molecules and the development of the convincing description of the dynamical changes in the electronic structure that occur in a chemical reaction.

A very significant and synthetic overview of the theoretical methods monitoring the series of events along IRC has been recently provided by Nanayakkar and Kraka.<sup>6</sup> The authors noticed two separate streams of efforts aiming at visualization of the bond formation/cleavage. They are based on observation of (i) potential energy surface (PES) and (ii) electron density (ED), respectively. According to Nanayakkar and Kraka PES derived schemes of studying chemical reactions are unified reaction valley approach (URVA) by Kraka and Cremer<sup>7–9</sup> and reaction fragility (RF) by Komorowski et al.<sup>10</sup> The authors demonstrate the general coherence between both URVA and RF leading to the quasi-spectral representation of the bond changes. However, electron density driven theories and results are based on the quantum theory of atoms-in-molecule method by Bader<sup>11</sup> (QTAIM) focused at the bond critical points for a series of reactions. A particularly interesting conclusion of this kind of study was the observation that no specific electron density

Received: October 7, 2019

Revised: December 7, 2019

Published: December 9, 2019



events have been associated with the observed reactions process at their transition states.<sup>12</sup> This tends to contradict the earlier results of the reaction force method (PES based) promoted by Toro-Labbé et al.<sup>13</sup> and by Politzer et al.,<sup>14</sup> indicating the region around TS as this reaction stage where the density changes might predominantly occur. There is another innovative approach derived from PES with the use reaction force surface by Dey and Shaw. They perform a simulation of a modified Hamilton–Jacobi equation and obtain wavefront–based formulation of reaction dynamics.<sup>15</sup>

Although our concept of the reaction fragility has been formally classified by Nanayakkar and Kraka as PES based,<sup>6</sup> the spectra represent a unique combination of information from PES and ED. Ordon et al.<sup>16</sup> has presented theoretical analysis illustrated by numerical results showing that RF spectra represent the electron density evolution in bond areas and thus reveal the mechanism of the reaction in terms of bond breaking and formation. The method stems from the conceptual density functional theory (c-DFT<sup>17–21</sup>). The framework of the c-DFT formalism has been developing over the years,<sup>22–27</sup> it is designed to describe the chemical reactivity of a molecule under external perturbations. Applications of the formalism founded on the Hohenberg–Kohn theorem<sup>28</sup> to chemical reactions have been driven by efforts to express the energy functional  $E_v[\rho(\mathbf{r})]$  as a functional of the external potential due to the nuclei, with the variations of the position of nuclei as working variables. The c-DFT approach to reactivity modifications along the IRC reaction path has recently proven its significance<sup>29–34</sup> and has been adopted to describe chemical reactions by using the nuclear coordinates,<sup>35–38</sup>  $\{\mathbf{R}\}$  rather than the local potential  $v(\mathbf{r})$  in chemical systems (molecules), as typically explored in the c-DFT consideration aimed at indexing the local reactivity in molecules.<sup>39–41</sup> The entire body of energy derivatives in the nuclear coordinate representations in a closed system ( $N, \{\mathbf{R}\}$ ) and open system ( $\mu, \{\mathbf{R}\}$ ) has been reviewed by Ordon et al.<sup>16,36</sup> as an alternative to the respective derivatives in the local representations recollected by Ayers et al.<sup>42</sup> The first energy derivative over  $\mathbf{R}_i$  represents the Hellmann–Feynman (H–F) force vector acting on a chosen nucleus:  $-\nabla_{\mathbf{A}}E$ . Consequently, second- and third-order derivatives are either numbers (e.g.,  $\nabla_{\mathbf{B}}\nabla_{\mathbf{A}}E = k_{\text{AB}}$ , force constant) or vectors (e.g.,  $\nabla_{\mathbf{A}}\mu = d(\nabla_{\mathbf{A}}E)/dN = -\Phi_{\mathbf{A}}$ , nuclear reactivity).<sup>36</sup> Third energy derivatives in the representation of nuclear coordinates have only rarely been focused on; the nuclear stiffness ( $\nabla_{\mathbf{A}}\eta = d^2(\nabla_{\mathbf{A}}E)/dN^2 = \mathbf{G}_{\mathbf{A}}$ ) has been proposed as a potential measure of the electron exchange perspective in a model colinear reaction.<sup>35</sup>

The third energy derivative with a considerable potential for description of changes occurring in a reacting system is the softness index  $\lambda$ , originally defined for a bond in a diatomic molecule,<sup>43</sup> then explored as a mode softening index,<sup>29</sup> and ultimately rigorously defined as a scalar softening index for a link AB:<sup>16</sup>  $[\nabla_{\mathbf{B}}\nabla_{\mathbf{A}}\mu]_N = [dk_{\text{AB}}/dN]_{\{\mathbf{R}\}} = \lambda_{\text{AB}}$ . Preliminary calculations of an average value of this index in a model reaction<sup>10</sup> have confirmed its high sensitivity to the local environment of atoms, as observed in the original work.<sup>43</sup>  $\lambda$  index exposes a sensitivity of a bond (its force constant) to the disturbance in  $N$ , occurring in a reaction.

This present work is aimed at developing a way to translate the information provided by the RF diagrams to the softening index,<sup>29</sup> quantitative parameter for potential use in chemistry. The natural target of the search is single H–X bond in environments allowing for proton exchange. The set of five

reactions involving a formamide structure have been selected for the test; they involve processes of the proton misplacement of much different nature: internal proton transfer, water mediated proton transfer, and double proton transfer in formamide dimer, as well as its sulfur analogues.

The choice of the formamide-type molecules as a model for the study of RF spectra is motivated not only by the rich information available for these molecules. Proton transfer (PT) reaction has long been recognized as crucial for explaining the tautomerization effects important in chemistry, in particular for biochemical activities of proteins or nucleic acids, and in further perspective, also for understanding the basic processes of life.<sup>44,45</sup> The cyclic formamide dimer has frequently been used as a model system for investigation proton transfer phenomena in the DNA bases pairs.<sup>46,47</sup> Parallel to the numerous computational studies on formamide dimer, also the proton migration in a monomeric formamide has been studied. Water mediated proton transfer in formamide has also been investigated extensively.<sup>48–52</sup> In the process of double proton transfer (DPT), the dimer assisted process has been found to be more favorable kinetically (lower energy barrier), while the water assisted process is characterized by lower reaction energy (endothermic).<sup>53,54</sup> Calculated energies have been found to be significantly dependent on the method and the basis set explored.<sup>55–59</sup> A separate chapter in these studies on proton transfer in the formamide containing systems is the energy decomposition.<sup>60,61</sup> The proton transfer in many double proton transfer reactions is unsymmetrical, leading to the molecules of much different chemical character from the reactants. Therefore, analysis of the reaction pathway allows for joint observation of the processes in two directions. The IRC studies by the DFT computational method have already been performed for the formamide dimer, its sulfur analogue and the corresponding mixed dimer.<sup>62–65</sup> The concerted, though not synchronous mechanism of the proton transfer has been suggested.<sup>66</sup>

## 2. METHOD

There is an increasing number of studies where c–DFT reactivity descriptors are used to explain experimental data.<sup>67,68</sup> Also, a renewed interest in extracting vital information from the Hellman–Feynman force concept (substantial for this present work) has been noticed.<sup>69</sup> Our goal in this present work is to come up with a new tool for such research—discovering factors that determine the intensity of the bands of RF spectra. An indirect information hidden in the spectra of bond fragilities is the bond energy change (increase or decrease) for a particular bond. The H–F force is by definition

$$-\nabla_{\mathbf{A}}E = \mathbf{F}_{\mathbf{A}} + \mathbf{F}_{\mathbf{A}}^{n-n} \quad (1)$$

$\mathbf{F}_{\mathbf{A}}^{n-n}$  stands for the nuclear repulsion force, and  $\mathbf{F}_{\mathbf{A}}$  is the electronic part:

$$\mathbf{F}_{\mathbf{A}} = \int \rho(\mathbf{r}) \mathbf{e}_{\mathbf{A}}(\mathbf{r}) d\mathbf{r} \quad (2)$$

The H–F force offers a remarkable potential for tracing the changes in a chemical reaction, as it is determined by the electron density function  $\rho(\mathbf{r})$  and the electrostatic field around an atom  $\mathbf{e}_{\mathbf{A}}(\mathbf{r})$  (eq 2). Its power has been exposed even further by exploring the vector representation; the second energy derivative of the nuclear repulsion term vanishes, as a consequence of the Laplace equation:  $\nabla_{\mathbf{B}}\cdot\mathbf{F}_{\mathbf{A}}^{n-n} = 0$ .<sup>16</sup> Hence, the divergence of force acting on a nucleus A

$(-\nabla_{\mathbf{B}} \cdot \nabla_{\mathbf{A}} E = \nabla_{\mathbf{B}} \cdot \mathbf{F}_{\mathbf{A}})$  is determined by the electron density function and the electric field of the nucleus  $\mathbf{e}_{\mathbf{A}}(\mathbf{r})$ , exclusively (eq 2). Moreover, since  $\nabla_{\mathbf{B} \neq \mathbf{A}} \cdot \mathbf{e}_{\mathbf{A}}(\mathbf{r}) = 0$ , an important relation has been demonstrated for the  $\nabla_{\mathbf{B} \neq \mathbf{A}} \cdot \mathbf{F}_{\mathbf{A}}$  derivative characterizing a link between atoms:<sup>16,70</sup>

$$\nabla_{\mathbf{B} \neq \mathbf{A}} \cdot \mathbf{F}_{\mathbf{A}} = \int \nabla_{\mathbf{B}} \rho(\mathbf{r}) \cdot \mathbf{e}_{\mathbf{A}}(\mathbf{r}) \, d\mathbf{r} \quad (3)$$

This finding has been fundamental for the proposed RF spectra technique. The divergence  $\nabla_{\mathbf{B}} \cdot \mathbf{F}_{\mathbf{A}} = k_{xx}^{\text{AB}} + k_{yy}^{\text{AB}} + k_{zz}^{\text{AB}}$  (cumulative force constant) represents the generalized analogue of the ordinary force constant (an element of the Hessian matrix)  $k_{ij}^{\text{AB}} = dF_{A,i}/dR_{B,j}$  ( $i, j = x, y, z$ ). The collection of divergences  $\nabla_{\mathbf{B}} \cdot \mathbf{F}_{\mathbf{A}}$  for all atoms in the system forms the  $(n \times n)$  connectivity matrix; its diagonal elements characterize atoms, and the off diagonal terms describe bonds and contacts between atoms.<sup>16,71</sup> An important feature of the proposed vector analysis is in providing an alternative to the normal-mode analysis of molecular vibrations. The scalar and invariant cumulative force constants  $\nabla_{\mathbf{B} \neq \mathbf{A}} \cdot \mathbf{F}_{\mathbf{A}}$  describe each particular bond with no other factors interfering.

The key effect in a molecule undergoing a chemical change is the electron density modification accompanying the displacement of nuclei. The effect of the reaction on the density can be monitored directly by the derivatives of the divergence of the H-F force (eq 3) over the reaction progress parameter ( $\xi$ ), since  $d\mathbf{e}_{\mathbf{A}}(\mathbf{r})/d\xi = 0$ . The routine quantum chemical computations dictate using the closed system ( $N=\text{const.}$ ), hence two types of derivatives have been introduced under the working labels of RF index for an atom  $a_{\xi}^{\text{AA}}$  and for a bond (or any other contact between atoms)  $a_{\xi}^{\text{AB}}$ .

$$a_{\xi}^{\text{AA}} \equiv \frac{d}{d\xi} [\nabla_{\mathbf{A}} \cdot \mathbf{F}_{\mathbf{A}}]_N \quad \text{and} \quad a_{\xi}^{\text{AB}} \equiv -\frac{d}{d\xi} [\nabla_{\mathbf{B} \neq \mathbf{A}} \cdot \mathbf{F}_{\mathbf{A}}]_N \quad (4)$$

The minus sign in  $a_{\xi}^{\text{AB}}$  is arbitrary; the derivatives are bound by the relation<sup>16,70,71</sup>

$$a_{\xi}^{\text{AA}} = \sum_{\mathbf{B} \neq \mathbf{A}} a_{\xi}^{\text{AB}} \quad (5)$$

The profiles of  $a_{\xi}^{\text{AA}}$  and  $a_{\xi}^{\text{AB}}$  along a reaction path reflect the electron density evolution in the reaction (RF spectrum for bonds or atoms).<sup>10,16,70,71</sup> Meaningful correlations with familiar quantities related to the electron density have been recently demonstrated:  $[\nabla_{\mathbf{B} \neq \mathbf{A}} \cdot \mathbf{F}_{\mathbf{A}}]_N$  was proved to correlate with the Wiberg bond order index ( $W_{\text{AB}}$ )<sup>70</sup> and  $[\nabla_{\mathbf{A}} \cdot \mathbf{F}_{\mathbf{A}}]_N$  with the atomic valence ( $V_{\mathbf{A}}$ ).<sup>71</sup> Hence, their derivatives demonstrated in RF spectra for bonds and atoms reproduce modifications in  $W_{\text{AB}}$  and  $V_{\mathbf{A}}$ , respectively, occurring in a reaction.

The intensity of peaks in the RF spectra needs an interpretation. Here we present analysis in the c-DFT language.

$$dk_{\text{AB}} = \left( \frac{\partial k_{\text{AB}}}{\partial N} \right)_{\{\mathbf{R}\}} dN + \sum_{\mathbf{C}} [\nabla_{\mathbf{C}} k_{\text{AB}}]_N \cdot d\mathbf{R}_{\mathbf{C}} \quad (6)$$

$dk_{\text{AB}}$  is infinitesimal change of the cumulative force constant within the  $\{\mathbf{R}\}$ ,  $N$  representation or canonical ensemble. For the reaction along IRC path the supermolecule does not change the total number of electrons and  $dN = 0$ . Also, an additional restriction applies: the change of nuclear coor-

dinates is limited to the identified minimum energy reaction trajectory (IRC). Hence, the unique variable parameter is sufficient to localize a system on IRC; the reaction progress ( $\xi$ ) replaces the whole set of nuclear coordinates  $\{\mathbf{R}\}$ . Equation 6 is reduced to

$$dk_{\text{AB}} = \sum_{\mathbf{C}} [\nabla_{\mathbf{C}} k_{\text{AB}}]_N \cdot d\mathbf{R}_{\mathbf{C}} = \left( \frac{\partial k_{\text{AB}}}{\partial \xi} \right)_N d\xi \quad (7)$$

The vector derivative in brackets (eq 6 and 7) has been identified and discussed previously.<sup>36,37</sup> For the closed system the cubic force constant (anharmonicity vector) is defined as

$$[\nabla_{\mathbf{C}} k_{\text{AB}}]_N = [\nabla_{\mathbf{C}} \cdot \nabla_{\mathbf{A}} \cdot \mathbf{F}_{\mathbf{B}}]_N \equiv \mathbf{a}_{\text{CAB}} \quad (8)$$

The conclusion from eq 7 is that only displacements of the nuclei matter for the bond RF profile  $a_{\xi}^{\text{AB}} = dk_{\text{AB}}/d\xi$  considered under the scrutiny of the closed system. Charge reorganization remains hidden in the anharmonicities characteristic for the closed system (eq 8). In order to expose role of density changes as separated from the displacements of the nuclei, the open system formalism must be explored. Here the variables for the differential are the chemical potential  $\mu$  and again the nuclear coordinates represented by the reaction progress  $\xi$ . The cumulative force constant  $\tilde{k}_{\text{AB}}$  in the open system is related to  $k_{\text{AB}}$ :<sup>36,37</sup>

$$\tilde{k}_{\text{AB}} = [\nabla_{\mathbf{B}} \cdot \mathbf{F}_{\mathbf{A}}]_{\mu} = k_{\text{AB}} - S\Phi_{\mathbf{A}} \cdot \Phi_{\mathbf{B}} \quad (9)$$

$S$  is global softness and  $\Phi_{\mathbf{A}} = -(dF_{\mathbf{A}}/dN)_{\mathbf{v}}$  stands for the nuclear reactivity vector.<sup>35</sup> The difference between  $\tilde{k}_{\text{AB}}$  and  $k_{\text{AB}}$  is due to the charge reorganization at the regime  $\mu = \text{const.}$  Considering the interaction of an atom  $\mathbf{A}$  with the remainder of a molecule we have,  $\tilde{k}_{\text{AA}} = k_{\text{AA}} - S\Phi_{\mathbf{A}}^2$  (eq 9). It is clear that the density adjustments in an open system make the cumulative force constant smaller:  $\tilde{k}_{\text{AA}} < k_{\text{AA}}$ .

The natural differential for  $\tilde{k}_{\text{AA}}$  in an open system along the reaction progress is

$$d\tilde{k}_{\text{AB}} = \tilde{\lambda}_{\text{AB}} d\mu + \left( \frac{\partial \tilde{k}_{\text{AB}}}{\partial \xi} \right)_{\mu} d\xi \quad (10)$$

The derivative in eq 10  $\tilde{\lambda}_{\text{AB}} = (\partial \tilde{k}_{\text{AB}} / \partial \mu)_{\xi}$  is the bond softening index in the open system;<sup>36,37</sup> the second term in eq 10 contains corresponding anharmonicities  $\tilde{\mathbf{a}}_{\text{CBA}} = [\nabla_{\mathbf{C}} \tilde{k}_{\text{AB}}]_{\mu}$  (cf. eqs 7 and 8). Given the relation between  $\tilde{k}_{\text{AB}}$  and  $k_{\text{AB}}$  (eq 9), the differential for  $k_{\text{AB}}$  is

$$dk_{\text{AB}} = d\tilde{k}_{\text{AB}} + d(S\Phi_{\mathbf{A}} \cdot \Phi_{\mathbf{B}}) \quad (11)$$

With eq 10 and also the established relation between the softening indices in open and closed systems,  $\tilde{\lambda}_{\text{AB}}$  and  $\lambda_{\text{AB}}$ , respectively,<sup>36,37</sup> final regrouping leads to the result

$$dk_{\text{AB}} = \lambda_{\text{AB}} S d\mu + \left( \frac{\partial k_{\text{AB}}}{\partial \xi} \right)_{\mu} d\xi \quad (12)$$

But also

$$dk_{\text{AB}} = \left( \frac{\partial k_{\text{AB}}}{\partial \mu} \right)_{\xi} d\mu + \left( \frac{\partial k_{\text{AB}}}{\partial \xi} \right)_{\mu} d\xi \quad (13)$$

Upon comparison of eq 12 and eq 13 the needed derivative is expressed by the bond softening index  $\lambda_{\text{AB}}$  for the closed system:

$$\left(\frac{\partial k_{AB}}{\partial \mu}\right)_{\xi} = \lambda_{AB} S \quad (14)$$

With the formal definition of the bond RF index (eq 4), the final result for  $a_{\xi}^{AB}$  as related to the bond softening index  $\lambda_{AB}$  is (from eq 13):

$$a_{\xi}^{AB} = \lambda_{AB} S J - \left(\frac{\partial k_{AB}}{\partial \xi}\right)_{\mu} \quad (15)$$

By standard definitions in the c-DFT formalism, the symbols in eq 15 are

$$\left(\frac{\partial k_{AB}}{\partial N}\right)_{\{R\}} = \lambda_{AB} \quad \text{bond softening index}^{29,36} \quad (16)$$

$$\left(\frac{\partial N}{\partial \mu}\right)_{\{R\}} = S \quad \text{global softness}^{17,23,24} \quad (17)$$

$$-\frac{d\mu}{d\xi} = J \quad \text{reaction electronic flux}^{72,73} \quad (18)$$

The bond RF index has been decomposed into two contributions (eq 15). The first comes from the change of the chemical potential at constant geometry (eq 13); thus it represents an effect of electron density change. The second term  $(\partial k_{AB}/\partial \xi)_{\mu}$  is monitoring a change due to the geometry variation only, with the chemical potential constant.

The softening index  $\lambda_{AB}$  (eq 16) is of particular interest. Within this formalism it may be defined for a contact between every two atoms, either bonded or merely interacting from a distance ( $A \neq B$ ) but also for an atom bound in a molecule as well ( $A = B$ ). Its meaning for a single atom ( $\lambda_{AA}$ ) is similar to that for a bond: the softening effect concerns the overall bonding of an atom to the rest of the system in question. The importance of this quantity is clearly seen, when an alternative c-DFT relation between  $k_{AB}$  for a bond ( $A \neq B$ ) and the electron density function is recalled (eq 4). By taking the derivative over  $N$  from eq 4, the direct relation for  $\lambda_{AB}$  is obtained:

$$\lambda_{AB} = \int \mathbf{e}_A(\mathbf{r}) \cdot [\nabla_{B \neq A} f(\mathbf{r})]_N d\mathbf{r} \quad (19)$$

$f(\mathbf{r})$  is the Fukui function:

$$f(\mathbf{r}) = \left[ \frac{\partial \rho(\mathbf{r})}{\partial N} \right]_{v(r)} \quad (20)$$

It has become evident that the electron density modifications occurring in a reaction must also be manifested in  $\lambda_{AB}$  (eq 19). Its role in determining the RF index for bonds and atoms (eq 15) can only be observed in the range, where it is not masked by the pure anharmonic effects in  $(\partial k_{AB}/\partial \xi)_{\mu}$ . The relation between the product ( $SJ$ ) along a reaction path and the RF spectrum of atoms and/or bonds ( $a_{\xi}^{AA}$ ,  $a_{\xi}^{AB}$ ) opens a way for determination of the softening index  $\lambda_{AA}$ ,  $\lambda_{AB}$  for the stable structures of reactants and products. The softening index for the reactant state (RS) and product state (PS) has been analyzed, focusing on the various X–H bonds in the systems chosen for this study; they are equivalent to the atomic softening indices for various hydrogens.

The practical meaning of the softening indices may also be assessed on the ground of c-DFT formalism. The atomic

softening index describes a response of the chemical potential of the system  $\mu$  to a virtual shift of an atom from its equilibrium position:<sup>16</sup>

$$\lambda_{AA} = \left(\frac{\partial k_{AA}}{\partial N}\right)_{\{R\}} = \nabla_A \cdot \nabla_A \mu \quad (21)$$

A displacement of an atom by  $\Delta \mathbf{R}_A$  in a closed system must result in a change in atomic populations, and specifically, it will result in some change  $\Delta N_A$ . For an average displacement of an atom in space we have  $\langle \delta \mathbf{R}_A \rangle = 0$  and  $\langle |\delta \mathbf{R}_A|^2 \rangle \neq 0$ . Hence, the virtual effect of a displacement of an atom  $\langle \delta \mathbf{R}_A \rangle$  on the chemical potential of the system can be approximated as

$$\langle \delta \mu \rangle = \frac{1}{2} \lambda_{AA} \langle |\delta \mathbf{R}_A|^2 \rangle \quad (22)$$

If the disturbed atom is considered as a separate system, and the reminder of a molecule as a reservoir of constant  $\mu$ , the virtual shift of an atom would not result in changing the chemical potential of the system ( $\langle \delta \mu \rangle = 0$ ), but rather in altering the population of this atom:

$$\eta \Delta N_A + \frac{1}{2} \lambda_{AA} \langle |\Delta \mathbf{R}_A|^2 \rangle = 0 \quad (23)$$

$\eta = 1/S$  is the global hardness of a system. Hence, the estimated change of the population on an atom responding to its average displacement is, approximately

$$\Delta N_A = -\frac{1}{2} \lambda_{AA} S \langle |\Delta \mathbf{R}_A|^2 \rangle \quad (24)$$

This result provides a meaning to the sign of the softening index, since  $S > 0$ . Atoms characterized with  $\lambda_{AA} > 0$  are supposed to dissociate with lowering their population  $\Delta N_A < 0$ ;  $\lambda_{AA} < 0$  implies the reverse effect. It is important to note that no definition for the atomic population has been implied by the above c-DFT analysis.

Theoretical analysis leads to the conclusion that two factors stimulate the intensity of the bond RF spectral peaks (eq 15): the first one represents the effect of the electron density reorganization in a system ( $\lambda_{AB} S J$ ), and the other  $(\partial k_{AB}/\partial \xi)_{\mu}$  reflects predominantly the structural change (anharmonicity). In the chosen proton transfer reaction, the structural changes do not play a substantial role: except for the shift of the hydrogen atom, other atoms do not move significantly from their original positions. Hence, modifications of bonds revealed by RF spectra of the heavy atoms reflect the electronic structure change in the system, induced by or causing the proton shift at some distance. By comparison of the small proton shift in dimers with the considerable proton moves in the monomeric formamide structure, the role of two components in eq 15 may be checked. Comparison between the oxygen and sulfur containing entities provides hints to the role of electronegativity of atoms involved.

### 3. COMPUTATIONAL DETAILS

Numerical results for the elements of the connectivity matrix have been obtained from the IRC energy profile reproduced by the standard procedure at the MP2 level using the 6-311++G(3df,3pd) basis set and the Gaussian 09 code.<sup>74</sup> The TS structures have been identified by means of the QST2 algorithm and verified with the frequency calculation for the normal vibrational modes. The reaction progress parameter ( $\xi$ ) has been calculated in the mass-weighted coordinates with

**Table 1.** Calculated Transition State Energies ( $\Delta E_{TS}$ ) and Reaction Energies ( $\Delta E$ ) for Proton Migration in Formamide Molecule (R1), Formamide/Water Complex (R2), Formamide Dimer (R3), Thioformamide Dimer (R4), and Formamide/Thioformamide Complex (R5)

molecule	no.	$\Delta E_{TS}$ [kcal/mol]	$\Delta E$ [kcal/mol]	refs
H <sub>2</sub> NCHO	R1	45.93	12.24	54, 48
(H <sub>2</sub> NCHO)·(H <sub>2</sub> O)	R2	22.14	10.63	54, 48
(H <sub>2</sub> NCHO) <sub>2</sub>	R3	19.95	18.58	63, 61, 56, 55
(H <sub>2</sub> NCHS) <sub>2</sub>	R4	30.54	27.08	63
(H <sub>2</sub> NCHO)·(H <sub>2</sub> NCHS)	R5	25.38	23.62	63

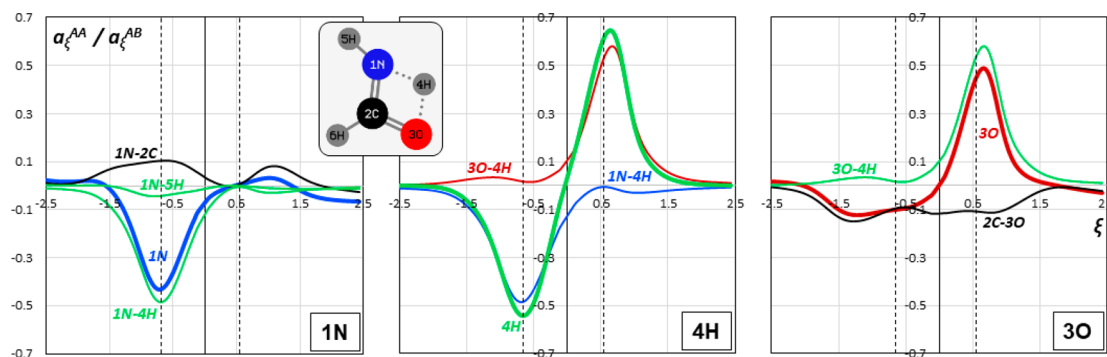


**Figure 1.** Reaction fragility (RF) spectra of atoms (eq 4, in au) for the proton migration in formamide molecule (R1): H<sub>2</sub>N—CH=O → HN=CH—OH. Decomposition into the RF bond profiles is shown for each atom (eq 5). Extreme points of the reaction force have been marked by the dashed lines at  $\xi = -0.67$  and  $\xi = +0.52$ .

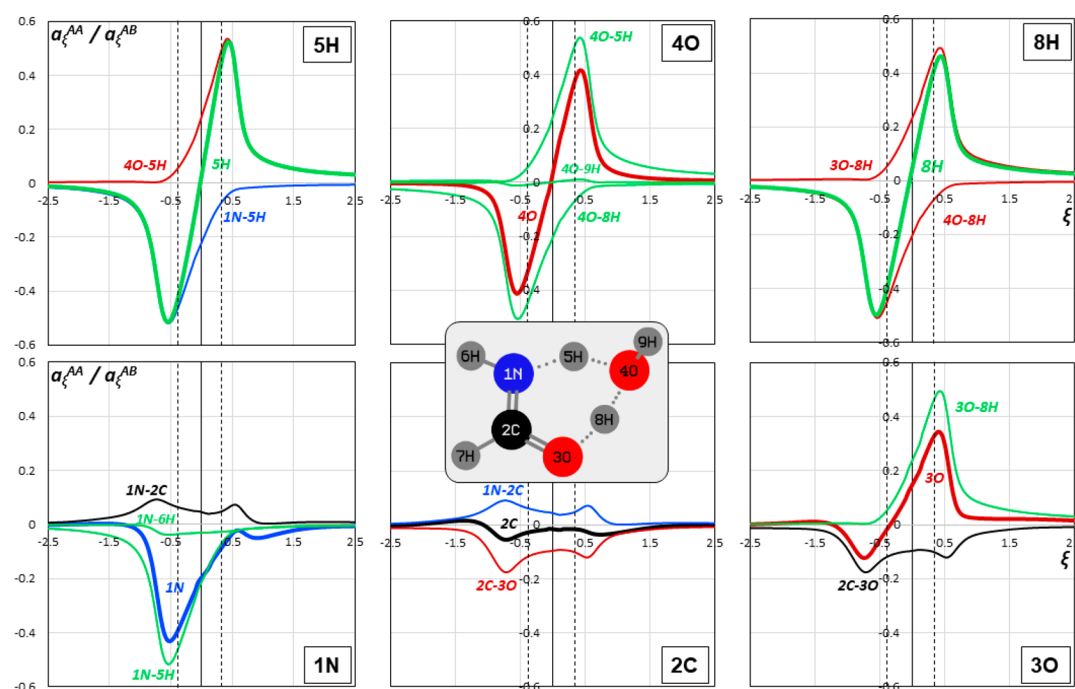


**Figure 2.** Reaction fragility (RF) spectra of both moving hydrogen atoms (5H, 8H) and of other atoms in the formamide/water complex izomerization by the proton transfer (R2): H<sub>2</sub>N—CH=O·H<sub>2</sub>O → HN=CH—OH·H<sub>2</sub>O ( $a_{\xi}^{AA}$  and  $a_{\xi}^{AB}$  in au). Decomposition into the RF bond profiles is shown for each atom (eq 5). Extreme points of the reaction force have been marked by the dashed lines at  $\xi = -0.41$  and  $\xi = 0.36$ .

a standard number about 150–200 points over each reaction path studied.<sup>3</sup> The Cartesian Hessian elements and the harmonic frequencies for the normal modes have been calculated for single points using the geometry of the structures resulting on the IRC. Proton transfer in the formamide molecule (R1) and in dimers (R3–R5) has been considered in the planar configuration, as established in the literature. For the formamide/water complex (R2), the most stable planar

configuration has been adopted with the second hydrogen atom in water molecule sticking out of the molecular plane. The structures of molecules undergoing a change have been envisaged in the figures corresponding to each reaction.

The results for the transition state energies ( $\Delta E_{TS}$ ) and the reaction energies ( $\Delta E$ ) in Table 1 reproduce quite accurately the data provided by other authors, indicated by citations in the last column. Since a variety of computational methods have

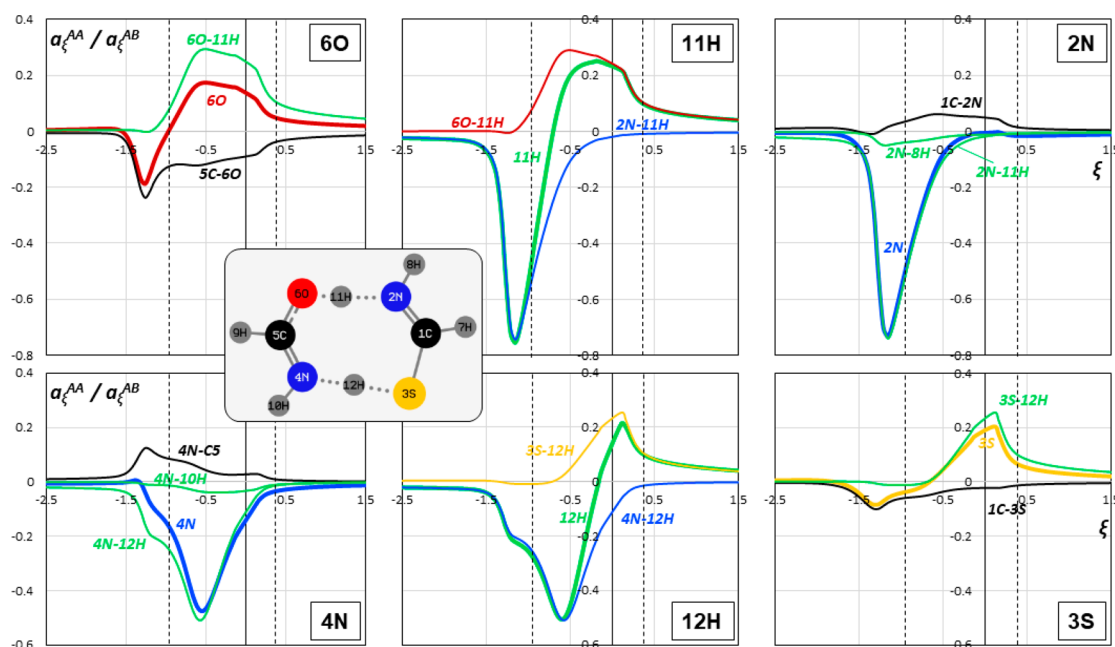


**Figure 3.** Reaction fragility (RF) spectrum of hydrogen atoms (center) moving between O and N atoms (upper row) and between N and S atoms (lower row) in the formamide/thioformamide complex upon the double proton transfer reaction (R5):  $\text{H}_2\text{N}-\text{CH}=\text{O} \cdot \text{H}_2\text{N}-\text{CH}=\text{S} \rightarrow \text{HN}=\text{CH}-\text{OH} \cdot \text{HN}=\text{CH}-\text{SH}$  ( $a_\xi^{\text{AA}}$  and  $a_\xi^{\text{AB}}$  in au). Decomposition into the RF bond profiles is shown for each atom (eq 5). Extreme points of the reaction force have been marked by the dashed lines at  $\xi_1 = -0.93$  and  $\xi_2 = +0.41$ .

been explored by the authors, the formamide tautomerization (R1) may serve for a benchmark of our method. MP2 results (with Dunning's "correlation consistent" polarized valence double- $\zeta$  bases) for this reaction by Wang et al.<sup>48</sup> are 45.2 and 11.8 kcal/mol for  $\Delta E_{\text{TS}}$  and  $\Delta E$  respectively, while Fu et al.<sup>54</sup> report MP2/6-311++g(2d,2p) corresponding data: 44.4 and 11.6 kcal/mol.

#### 4. RESULTS AND DISCUSSION

Examples of the spectra for proton migration processes have been shown with appropriate comments below. It has been found in the previous study, that the bond RF spectra very accurately indicate the bond changes as measured by the Wiberg bond order indices  $W_{\text{AB}}$ .<sup>70,71,75</sup> Consequently, the phrases "bond order increase" and "bond order decrease" will be used to describe the upward and downward peaks in bond fragilities, respectively.

**Reaction Fragility (RF) Spectra for Atoms and Their Bonds.** Examples of the RF spectra for atoms  $a_\xi^{\text{AA}}$  and bonds  $a_\xi^{\text{AB}}$  have been presented for the three characteristic types of reactions: R1, R2, and R5. Additional spectra for reactions R3 and R4 may be found in the Supporting Information. For the sake of clarity, the range of the reaction progress  $\xi$  has been limited to the regions where nontrivial peaks are observed. The central region around the transition state (TS,  $\xi = 0$ ) has been marked by the dashed lines at points of the extreme reaction force  $F_\xi = -dE/d\xi$ , as proposed by Toro-Labbé et al.<sup>76</sup>

**Characteristics (Figure 1).** The first step in bond reorganization is observed at ca.  $\xi \cong -2.0$  by the C=O bond order decrease (3O) and C—N bond order increase (1N) with only a minor change in O—H bond order as the hydrogen is initially shifted away from N (3O, 4H). This may be considered as the polarization effect: the progress in increasing the O—H bond order stops at ca.  $\xi \cong -1.1$  and will not continue until the C—N bond reaches its maximum point (ca.  $\xi_1 \cong -0.6$ ). The N—H bond breaks entirely at

ca.  $\xi \cong +0.6$  and only then does the O—H bond reach its peak (ca.  $\xi \cong +0.7$ ); increasing the C—O bond order follows. The last step of the reaction is some additional C—N bond increase (ca.  $\xi_1 \cong +1.0$ ) along with the final accent in breaking the N—H bond. The role of the carbon atom is reflected by the C—N and C—O bond lines (1N and 3O); the carbon atom loses its bond to oxygen, but this is compensated by increasing the bond to nitrogen. The most pronounced peaks of the RF spectra are those for hydrogen abstraction from the nitrogen and its attachment to the oxygen atom, their positions coincide approximately with the extreme points of the reaction force, while the electron density flow between C—N and C—O bonds occurs in a much wider range of reaction progress ( $-2 < \xi < +2$ ).

**Characteristics (Figure 2).** The atomic RF spectra for both moving hydrogens are fully symmetric (5H, 8H); they represent a synchronous exchange processes of proton shifts between the formamide and assisting water molecule. The symmetric atomic peaks for oxygen atom (4O) confirm this conclusion. The 9H hydrogen atom in water is but a spectator in this process, as testified by the 9H—4O RF bond index. The onset of the proton transfer is observed as early as at ca.  $\xi \cong -2.0$  (5H, 4O, 8H, 1N). Very interestingly, the 3O—8H bond does not form until ca.  $\xi \cong -0.6$  (8H, 3O) and it is clearly preceded by the 2C—3O bond order decrease at ca.  $\xi \cong -1.6$  (3O, 2C); this occurs parallel to the increase of 2C—1N bond order (1N, 2C). An interesting conclusion: polarization of the formamide N—C—O backbone due to the initial 5H shift toward 4O occurs first, and the intercept of 8H by 3O comes as a result.

**Characteristics (Figure 3).** In order to expose the difference between the hydrogen movements in formamide  $\text{N}-\text{H} \cdots \text{O} \rightarrow \text{N} \cdots \text{H}-\text{O}$  and thioformamide  $\text{N}-\text{H} \cdots \text{S} \rightarrow \text{N} \cdots \text{H}-\text{S}$  only RF spectra of atoms directly participating in this process have been collected in Figure 3, together with RF spectra of their bonds. The hydrogen spectra reveal a

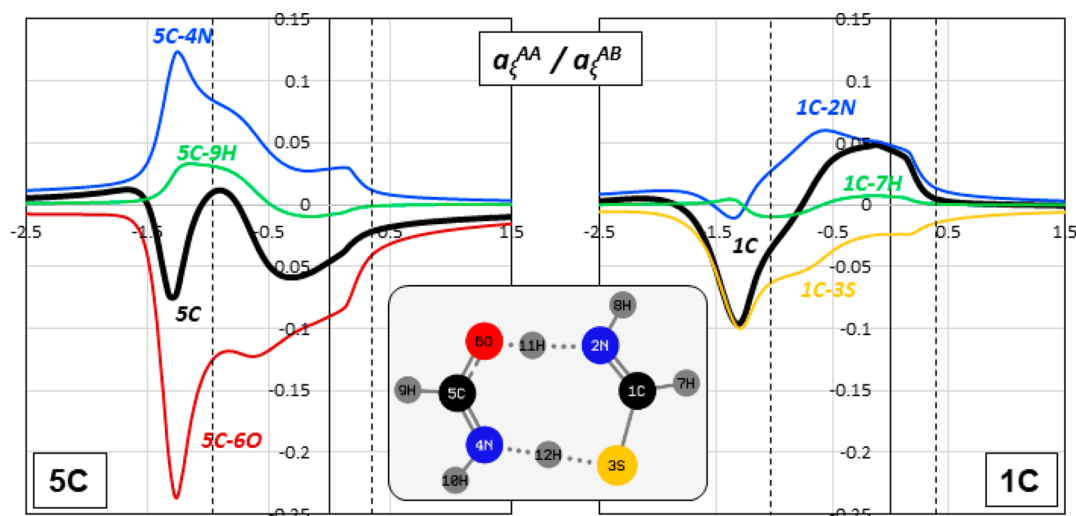


**Figure 4.** Reaction fragility (RF) of carbon atoms in the formamide/thioformamide complex upon the double proton transfer reaction (R5):  $\text{H}_2\text{N}-\text{CH}=\text{O} \cdot \text{H}_2\text{N}-\text{CH}=\text{S} \rightarrow \text{HN}=\text{CH}-\text{OH} \cdot \text{HN}=\text{CH}-\text{SH}$  ( $a_{\xi}^{\text{AA}}$  and  $a_{\xi}^{\text{AB}}$  in au). Decomposition into the RF bond profiles is shown (eq 5). Extreme points of the reaction force have been marked by the dashed lines at  $\xi_1 = -0.93$  and  $\xi_2 = +0.41$ .

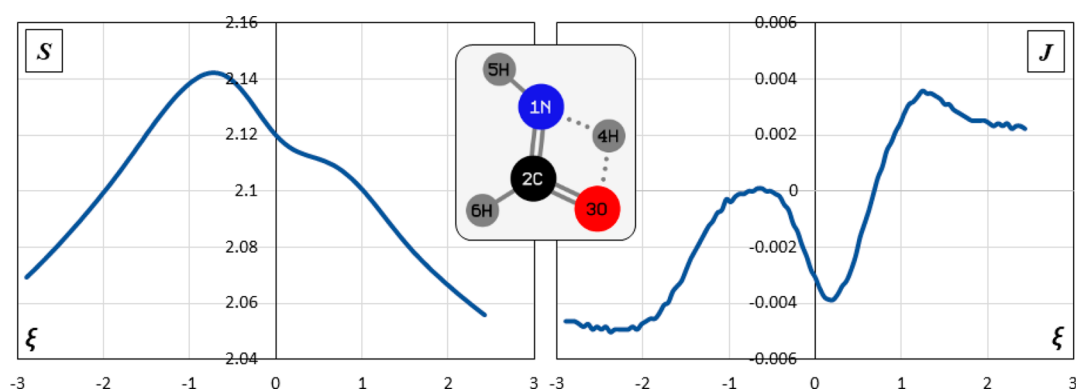


**Figure 5.** Global softness  $S$  (eq 25) and reaction electronic flux (eqs 18 and 25) for proton migration in formamide (R1) [au].

correlation between the two shifts: both start at ca.  $\xi \cong -1.6$  with breaking the N–H bonds (11H and 12H). In  $\text{N}-\text{H} \cdots \text{O}$  the N–H bond breaks early (at ca.  $\xi \cong -1.2$ , 11H) and this is also marked on the N–H peak within  $\text{N}-\text{H} \cdots \text{S}$  (12H). Actual breaking of the N–H bond in  $\text{N}-\text{H} \cdots \text{S}$  comes only at ca.  $\xi \cong -0.6$ . Formation of the O–H and S–H bonds starts only when the fragilities for corresponding N–H bonds reach their extrema at  $\xi \cong -1.2$  and  $\xi \cong -0.6$ , respectively (11H and 12H). The maxima of bond fragilities for O–H and S–H bonds appear at  $\xi \cong -0.5$  and  $\xi \cong +0.15$ , respectively. The wide shoulder in O–H peak (6O and 11H) and also in 6O and 11H peaks (6O and 11H, respectively) indicate to a possible coupling with the concerted move of 12H toward 3S and the S–H bond formation in this region (3S and 12H).

**Characteristics (Figure 4).** There is a well illustrated fact that strong bonds of oxygen atoms produce stronger and sharper peaks than similar weak bonds of sulfur atom.

The RF spectra of carbon atoms in the center of the monomer backbone are most interesting, as they reveal a notable difference between the  $\text{H}_2\text{N}-\text{CH}=\text{O}$  and  $\text{H}_2\text{N}-\text{CH}=\text{S}$  molecules. The density shift from the  $\text{C}=\text{O}$  bond to the  $\text{C}-\text{N}$  bond is clearly manifested by peaks at ca.  $\xi \cong -1.2$  (5C), when the distant  $2\text{N}-11\text{H}$  bond is fully broken (Figure 3: 11H) and the closer  $4\text{N}-12\text{H}$  bond tends to follow (Figure 3: 12H); the RF profile of the 5C carbon

atom (5C) shows a balance between these two processes. The second stage of the reaction is the  $6\text{O}-11\text{H}$  bond formation at ca.  $\xi \cong -0.5$  (Figure 3: 11H); this is accompanied by the completion of the  $4\text{N}-12\text{H}$  bond rupture (Figure 3: 12H). At this point, the 5C carbon suffers for some density loss (5C) to the oxygen atom (Figure 3: 6O). Parallel to the density evolution in the formamide molecule, the thioformamide molecule survives quite different events. The first sign of a change comes only when the 12H drifts apart from 4N, but well before this bonds breaks (Figure 3: 12H, shoulder at  $\xi \cong -1.2$ ). In this very moment, the  $1\text{C}-3\text{S}$  bonds breaks entirely (1C). This must be interpreted as the result of polarization the  $1\text{C}-3\text{S}$  bond by the approaching hydrogen (12H), since the density flow from the  $\text{C}=\text{S}$  to the  $1\text{C}-2\text{N}$  bond will not come until ca.  $\xi \cong -0.5$  (1C), and the  $3\text{S}-12\text{H}$  bond will be formed even later at ca.  $\xi \cong 0.2$  (Figure 3: 3S). This conclusion gets support from observation of the RF profile of nitrogen atoms 4N (in formamide) and 2N (in thioformamide). The  $5\text{C}-4\text{N}$  bond gets stronger when the  $5\text{C}-6\text{O}$  bond order decreases with 11H approaching 6O (5O); approaching 12H to 3S atom has little effect on  $1\text{C}-2\text{N}$  bond.

**Calculation of the Atomic Softening Indices.** The relation between the atomic RF index  $a_{\xi}^{\text{AA}}$  and atomic softening index  $\lambda_{\text{AA}}$  given by eq 15 has been tested numerically. The

Table 2. Calculated Softening Indices  $\lambda_{\text{HH}}$  for Hydrogen Atoms in the Stationary Configurations of the Reactant (RS) and Product (PS)<sup>a</sup>

reaction	$\Delta\xi^b$	$R^2^c$	$\sum_A(\partial k_{\text{AA}}/\partial\xi)_\mu^c$	$\lambda_{\text{HH}}$ for H atoms in H-(H)N-(H)C-(X)-H			
				H-(HN)-	-(H)N-	-(H)C-	-(X)-H
R1	RS (-2.85; -2.4)	0.711	-0.64	1.76	1.04	-1.15	
	PS (1.85; 2.4)	0.700	0.62		0.20	-0.39	9.32
R2	RS (-4.0; -3.5)	0.954	0.02	-1.27	-0.04	0.31	-2.39 /c
	PS (2.5; 3.0)	0.909	-0.07	-7.60 <sup>d</sup>	0.15	0.14	-6.62
R3	RS (-4.5; -3.5)	0.870	0.03	4.53	0.11	-0.14	
	PS (0.5; 1.5)	0.924	0.05		-1.22	1.30	37.80
R4	RS (-5.4; -4.4)	0.714	0.03	-3.43	-0.26	0.07	
	PS (2.0; 4.0)	0.734	0.004		-0.43	-0.21	14.10
R5 (X = O)	RS (-4.0; -5.0)	0.886	0.05	2.76	0.15	-0.16	
	PS (1.5; 2.5)	0.949	0.07		-0.21	0.15	10.94
R5 (X = S)	RS (-4.0; -5.0)	0.886	0.05	3.47	0.14	0.03	
	PS (1.5; 2.5)	0.949	0.07		-0.33	-0.11	10.30

<sup>a</sup>The data for the moving hydrogen atoms have been indicated at the end of the N-C-X backbone, at N and X = O, S atoms, for the initial and final phases of reactions, respectively. All data are in [au]. <sup>b</sup>RS, reactant state. PS, product state. <sup>c</sup>Global correlation  $a_\xi = \sum a^{\text{AA}}$  vs  $SJ$  (eq 15). <sup>d</sup>In water molecule. Also, for the inactive -O(H) atom:  $\lambda_{\text{HH}} = -0.15$  (RS),  $\lambda_{\text{HH}} = -0.41$  (PS).

evolution of global softness ( $S$ , eq 17) and the reaction electronic flux ( $J$ , eq 18) has been shown in Figure 5 for the proton migration in formamide as characteristic example. The HOMO and LUMO orbital energies have been calculated on each step of the reaction and served as a source for calculation of global softness ( $S$ ) and the chemical potential ( $\mu$ ), necessary for calculation of the reaction electronic flux ( $J$ , eq 18).

$$S = (\varepsilon_{\text{LUMO}} - \varepsilon_{\text{HOMO}})^{-1} \quad \text{and} \quad \mu = \frac{1}{2}(\varepsilon_{\text{LUMO}} + \varepsilon_{\text{HOMO}}) \quad (25)$$

The total variation of softness  $S$  in this reaction does not exceed 0.1 au and variation in  $J = -d\mu/d\xi$  is less than 0.01 au (Figure 5). This range is typical and has been observed by other authors also for the double proton transfer in formamide dimer.<sup>63</sup> The typical variation range of atomic RF index (ca. 1 au) is by one order of magnitude larger. This indicates that the atomic RF index value in eq 15 may be controlled mainly by the variation of  $\lambda$ , only the role of the  $(\partial k_{\text{AA}}/\partial\xi)_\mu$  derivative must be checked.

The following procedure has been adopted. To determine  $\lambda_{\text{AA}}$  for atoms in the reactants state (RS), the linear correlation between  $a_\xi^{\text{AA}}$  and  $SJ$  has been checked for a series of initial reaction steps, where the RF spectrum remains flat. The range has been gradually extended, until the deterioration of the linear correlation (measured by  $R^2$  value) has been observed. The procedure was repeated for the final flat part of each spectrum leading to the  $\lambda_{\text{AA}}$  parameters for atoms in the (PS) structure. The resulted range  $\Delta\xi$  as well as  $R^2$  values have been collected in Table 2 together with final correlation parameters  $\lambda_{\text{AA}}$  (slope). The  $(\partial k_{\text{AA}}/\partial\xi)_\mu$  term in eq 15 has been found small for all atoms and bonds, and therefore, only its global value summed for all atoms has been reported in Table 2. The results have been presented for all hydrogen atoms as characteristic examples; they allow for preliminary assessment of actual meaning of the softening indices for atoms resulting in the adopted procedure. The  $\lambda_{\text{AA}}$  indices for hydrogens in all systems are equivalent to the  $\lambda_{\text{AB}}$  index for the X-H bond.

The data in Table 2 expose some characteristic trends. The anharmonicity term  $\sum_A(\partial k_{\text{AA}}/\partial\xi)_\mu$  (eq 15) is small for all reactions; however, it is considerably larger for R1 than for other reactions. The proton migration in formamide requires

bending of the H-N bond, before the H proton can be moved to create the H-O bond; this has been recognized as the main reason for extremely high TS energy in this reaction<sup>48</sup> and is corroborated by the relatively large value of the derivative  $(\partial k_{\text{AA}}/\partial\xi)_\mu$  in Table 2. In other reactions, this parameter has been found negligibly small, which corresponds to the chemical intuition: neither the proton shift between the formamide and water molecule, nor the double proton transfer in dimers requires substantial bond bending.

Basic properties of  $\lambda_{\text{HH}}$  indices can be discussed from inspection of Table 2. The vital approximation (eq 23) is most natural for the hydrogen atoms and only hydrogen atoms considerably change their position in the reactions studied. Assessing whether a proton dissociation is cationic ( $\lambda_{\text{AA}} > 0 \rightarrow \Delta N_{\text{A}} < 0$ ) or anionic ( $\lambda_{\text{AA}} < 0 \rightarrow \Delta N_{\text{A}} > 0$ ) may be of practical importance.

The softening indices for the inactive hydrogen atoms -(H)N- and -(H)C- and also for the inactive -O(H) atom in water molecule are small, and only slightly variable between RS and PS. However, the softening index for the acidic -(X)-H atoms are all positive and relatively high, depending both on the nature of the connected atom (X = S in R4, R5; X = O in R1, R2, R3, R5) and on the nature of the reaction path.

Although H-(HN)- and -(H)N- hydrogen atoms in  $\text{NH}_2$  group are formally identical in RS of all systems, their  $\lambda_{\text{HH}}$  indices are not; apparently, they reflect various environments. The same effect is observed for the two hydrogen atoms in a water molecule (R2: RS and PS). Protons moving from the N atom (basic and more stable) to the X (O, S) atom (acidic and less stable) increase their softening index by an order of magnitude or more (R3). Hydration of the  $\text{H}_2\text{NCHO}$  molecule dramatically changes the softening indices for both hydrogens to be exchanged with the  $\text{H}_2\text{O}$  molecule (R2); their  $\lambda_{\text{AA}}$  indices are lowered with respect to their initial situation. The acidic -(X)-H hydrogen atoms (PS) are characterized by positive  $\lambda_{\text{HH}}$  indices that are regularly higher than the index for the amide group H-(HN)- hydrogen atoms in the same system.  $\lambda_{\text{HH}}$  indices for this type of hydrogen atom are all positive, as expected for the cationic detachment of -(X)-H hydrogen from the N-C-X backbone.

In the presence of water, the end hydrogen atom H-(HN)- changes its status by interaction with the molecule of water

(R2 vs R1); its  $\lambda_{\text{HH}}$  becomes negative (−1.27 vs +1.76). The  $\lambda_{\text{HH}}$  index gets even more negative when this atom is shifted toward the oxygen atom in H<sub>2</sub>O (−1.27 to −7.60). The −(O)–H hydrogen being detached from H<sub>2</sub>O undergoes an analogous change upon shift (−2.39 to −6.62). The presence of a water molecule radically modifies properties of the hydrogen atoms in the vicinal monomer, they gain some population upon detachment.

A valuable test is provided by the H–(HN)– hydrogen atoms in formamide (R3: RS,  $\lambda_{\text{HH}} = 4.53$ ) and thioformamide (R4: RS,  $\lambda_{\text{HH}} = -3.43$ ). In R3 the hydrogen atom is expected to lose its population (eq 24) when abstracted from nitrogen, while in thioformamide it should gain electrons in the same process. This indeed is readily understood by the significantly lower electronegativity of sulfur atom as compared to oxygen; the N–C–O backbone is more polarized than N–C–S, as observed on the RF spectra.

The  $\lambda_{\text{HH}} = 37.8$  index for the hydrogen atom −(O)–H at another end of the formamide type skeleton in R3 (PS) indicates that it can only be abstracted, leaving its electron behind that meaning proton dissociation, while the effect for the R4 (PS) −(S)–H hydrogen atom is considerably weaker ( $\lambda_{\text{HH}} = 14.4$ ). This observation is well in accord with the known properties of the OH vs SH compounds: the OH hydrogen is typically more acidic than SH, and the formamidine molecule HN=CH–OH (PS state in R3) is occasionally called a formamidic acid.<sup>54</sup>

## 5. CONCLUSIONS

We present an analysis based on the concept of the reaction fragility (RF) resulting in a novel approach to evaluate the numerical bond softening index  $\lambda_{\text{AB}}$ . The bond softening index is designated to reveal how much of the force constant is being lost with the electron transferred to/from a molecule. The basic theoretical result is eq 15, which exposes a relation between the c-DFT descriptors ( $S$ ,  $J$ ,  $\lambda_{\text{AB}}$ ) and the calculated intensity of the bond RF spectrum ( $a_{\text{e}}^{\text{AB}}$ ). Furthermore, we present arguments that  $\lambda_{\text{AB}}$  provides the most significant contribution into the RF index  $a_{\text{e}}^{\text{AB}}$ . We used eq 15 to determine the approximate values of the bond softening indices  $\lambda_{\text{AB}}$  for the equilibrium structures (RS, PS). The softening indices for X–H bonds properly reflect the acidity of attached protons and are extremely sensitive to the local environment of a bond, thus opening a perspective for testing the  $\lambda_{\text{AB}}$  indices as reactivity indices; consequently, the bond index  $\lambda_{\text{AB}}$  has been generalized to bonded atoms  $\lambda_{\text{AA}}$  (eq 21). The atomic softening index  $\lambda_{\text{AA}}$  provides a rough measure of the sensitivity of the electronic population of that atom, to its virtual displacement from the equilibrium position (eq 24). Equation 15, presenting a formal proof for the connection of the intensity of peaks in the RF profiles to the corresponding softening indices (either for bonds or for atoms), discloses the deep content of these diagrams. They describe predominantly the local change hidden within  $\lambda$  index, while the variation of global parameters ( $S$ ,  $J$ ) is playing a minor role. The presented justification for the connection between  $\lambda$  and the direction and the degree of change in population for an atom (eq 24) opens a wide field for explorations potentially useful in practical chemistry.

However, eq 19 shows that  $\lambda_{\text{AB}}$  is another nuclear reactivity index as are  $\Phi_{\text{A}}$  and  $G_{\text{A}}$ .<sup>77,29,35,38</sup> Usually the reactivity index is designated to give desired information without actually performing calculations of the trajectory of the chemical

reaction. The Fukui function gives information on how much electron density increases or decreases at point  $r$ , if the total number of electrons is changed by one. The bond softening index gives the force constant change with respect to the total number of electrons. Such prediction determines if the particular bond is a substantial subject of the reaction or is an observer. Here we present the computational scheme for obtaining the bond softening index from the concept of the RF spectrum along IRC reaction path calculations. This fact validates strongly the significance of the concept reaction fragility spectra

By describing the dynamical changes in local properties (bonds, atoms) on the grounds of the well-defined physical quantity (Hellmann–Feynman force on the nuclei), with no need for the specific and always arbitrary density separation between atoms, the RF spectra respond, in a way, to the question recently raised by Politzer and Murray in their deep discussion: *A Look at Bonds and Bonding*.<sup>78</sup> “As far as chemistry is concerned, the key questions are more practical than a formal distinction between bond and bonding, e.g.: How strongly is an atom held in a system? To what extent is its situation modified upon a reaction? How are the variations in bonding status of atoms interconnected?” By calculating the atomic softening indices, we have demonstrated how monitoring a reacting system by the RF spectra technique provides spectacular answers to these questions.

## ■ ASSOCIATED CONTENT

### Supporting Information

The Supporting Information is available free of charge at <https://pubs.acs.org/doi/10.1021/acs.jpca.9b09426>.

Presentation and discussion of the fragility spectra for the double proton transfer reactions in (H<sub>2</sub>N–CHO)<sub>2</sub> and (H<sub>2</sub>N–CHS)<sub>2</sub> dimers (R3 and R4) (PDF)

## ■ AUTHOR INFORMATION

### Corresponding Author

\*E-mail: [piotr.ordon@upwr.edu.pl](mailto:piotr.ordon@upwr.edu.pl).

### ORCID

Piotr Ordon: 0000-0002-7136-0367

Jarosław Zaklika: 0000-0002-1322-4148

Mateusz Jędrzejewski: 0000-0002-0467-5086

Ludwik Komorowski: 0000-0003-2807-8101

### Notes

The authors declare no competing financial interest.

## ■ ACKNOWLEDGMENTS

The use of resources of Wrocław Center for Networking and Supercomputing is gratefully acknowledged (WCSS Nos. 249 and GW 036).

## ■ REFERENCES

- (1) Fukui, K. The Path of Chemical Reactions - the IRC Approach. *Acc. Chem. Res.* **1981**, *14*, 363–368.
- (2) Miller, W. H.; Handy, N. C.; Adams, J. E. Reaction Path Hamiltonian for Polyatomic Molecules. *J. Chem. Phys.* **1980**, *72*, 99–112.
- (3) Piela, L. *Ideas of Quantum Chemistry*; Elsevier: Amsterdam, 2007.
- (4) Klippenstein, S. J.; Pande, V. S.; Truhlar, D. G. Chemical Kinetics and Mechanisms of Complex System: A Perspective on Recent Theoretical Advances. *J. Am. Chem. Soc.* **2014**, *136*, 528–546.

- (5) López, J. G.; Vayner, G.; Lourderaj, U.; Addepalli, S. V.; Kato, S.; deJong, W. A.; Windus, T. L.; Hase, W. L. A Direct Dynamics Trajectory Study of  $F^- + CH_3OOH$  Reactive Collisions Reveals a Major Non-IRC Reaction Path. *J. Am. Chem. Soc.* **2007**, *129*, 9976–9985.
- (6) Nanayakkara, S.; Kraka, E. A New Way of Studying Chemical Reactions: a Hand-in-hand URVA and QTAIM Approach. *Phys. Chem. Chem. Phys.* **2019**, *21*, 15007–15018.
- (7) Kraka, E.; Cremer, D. Characterization of CF Bonds with Multiple-Bond Character: Bond Lengths, Stretching Force Constants, and Bond Dissociation Energies. *ChemPhysChem* **2009**, *10*, 686–698.
- (8) Kraka, E.; Cremer, D. Computational Analysis of the Mechanism of Chemical Reactions in Terms of Reaction Phases: Hidden Intermediates and Hidden Transition States. *Acc. Chem. Res.* **2010**, *43*, 591–601.
- (9) Zou, W.; Sexton, T.; Kraka, E.; Freindorf, M.; Cremer, D. A New Method for Describing the Mechanism of a Chemical Reaction Based on the Unified Reaction Valley Approach. *J. Chem. Theory Comput.* **2016**, *12*, 650–663.
- (10) Komorowski, L.; Ordon, P.; Jędrzejewski, M. The Reaction Fragility Spectrum. *Phys. Chem. Chem. Phys.* **2016**, *18*, 32658–32663.
- (11) Bader, R. F. W. *Atoms in Molecules. A Quantum Theory*; Clarendon Press: Oxford, U.K., 1990.
- (12) Sexton, T.; Kraka, E.; Dieter Cremer, D. Extraordinary Mechanism of the Diels–Alder Reaction: Investigation of Stereochemistry, Charge Transfer, Charge Polarization, and Biradicaloid Formation. *J. Phys. Chem. A* **2016**, *120*, 1097–1111.
- (13) Toro-Labbé, A.; Gutiérrez-Oliva, S.; Politzer, P.; Murray, J. S. Reaction Force: A Rigorously Defined Approach to Analyzing Chemical and Physical Processes. In *Chemical Reactivity Theory. A density functional Viewpoint*; Chattaraj, P. K., Ed.; CRC Press, Taylor & Francis Group: Boca Raton, FL, 2009.
- (14) Politzer, P.; Toro-Labbé, A.; Gutiérrez-Oliva, S.; Murray, J. S. In *Perspectives on the Reaction Force in Advances in Quantum Chemistry*; Sabin, J. R., Brändas, E. J., Eds.; Elsevier: Amsterdam, 2012; Vol. 64.
- (15) Dey, B. K.; Shaw, S. Reaction Force Surface for the Hydrogen Transfer Reaction in Malonaldehyde: A Classical Wavefront-based Formulation. *J. Theor. Comput. Chem.* **2018**, *17*, 1850051.
- (16) Ordon, P.; Komorowski, L.; Jędrzejewski, M. Conceptual DFT Analysis of the Fragility Spectra of Atoms Along the Minimum Energy Reaction Coordinate. *J. Chem. Phys.* **2017**, *147*, 134109.
- (17) Parr, R. G.; Yang, W. *Density-Functional Theory of Atoms and Molecules*; Oxford University Press, Oxford, U.K., 1989.
- (18) Parr, R. G.; Donnelly, R. A.; Levy, M.; Palke, W. E. Electronegativity: The Density Functional Viewpoint. *J. Chem. Phys.* **1978**, *68*, 3801–3807.
- (19) Parr, R. G.; Pearson, R. G. Absolute Hardness: Companion Parameter to Absolute Electronegativity. *J. Am. Chem. Soc.* **1983**, *105*, 7512–7516.
- (20) Parr, R. G.; Yang, W. Density Functional Approach to the Frontier-electron Theory of Chemical Reactivity. *J. Am. Chem. Soc.* **1984**, *106*, 4049–4050.
- (21) Berkowitz, M.; Ghosh, S. K.; Parr, R. G. On the Concept of Local Hardness in Chemistry. *J. Am. Chem. Soc.* **1985**, *107*, 6811–6814.
- (22) Nalewajski, R. F. A Coupling Between the Equilibrium State Variables of Open Molecular and Reactive Systems. *Phys. Chem. Chem. Phys.* **1999**, *1*, 1037–1049.
- (23) Geerlings, P.; De Proft, F.; Langenaeker, W. Conceptual Density Functional Theory. *Chem. Rev.* **2003**, *103*, 1793–1874.
- (24) Chermette, H. Chemical Reactivity Indexes in Density Functional Theory. *J. Comput. Chem.* **1999**, *20*, 129.
- (25) Ordon, P. *Ph.D. Thesis*, Wrocław University of Technology, 2003.
- (26) Balawender, R.; Geerlings, P. Nuclear Fukui Function from Coupled Perturbed Hartree–Fock Equations. *J. Chem. Phys.* **2001**, *114*, 682.
- (27) Szarek, P.; Witkowski, M.; Wozniak, A. P. Unconventional Look at the Diameters of Quantum Systems: Could the Characteristic Atomic Radius Be Interpreted as a Reactivity Measure? *J. Phys. Chem. C* **2019**, *123*, 11572–11580.
- (28) Hohenberg, P.; Kohn, W. Inhomogeneous Electron Gas. *Phys. Rev.* **1964**, *136*, B864.
- (29) Ordon, P.; Tachibana, A. Use of Nuclear Stiffness in Search for a Maximum Hardness Principle and for the Softest States Along the Chemical Reaction Path: A New Formula for the Energy Third Derivative  $\gamma$ . *J. Chem. Phys.* **2007**, *126*, 234115.
- (30) Ordon, P.; Tachibana, A. Nuclear Reactivity Indices Within Regional Density Functional Theory. *J. Mol. Model.* **2005**, *11*, 312–316.
- (31) Jędrzejewski, M.; Ordon, P.; Komorowski, L. Variation of the Electronic Dipole Polarizability on the Reaction Path. *J. Mol. Model.* **2013**, *19*, 4203–4207.
- (32) Jędrzejewski, M.; Ordon, P.; Komorowski, L. Atomic Resolution for the Energy Derivatives on the Reaction Path. *J. Phys. Chem. A* **2016**, *120*, 3780–3787.
- (33) Neelamraju, V. S. K.; Jaganade, T. A Reaction Force Perspective of a Model Amide Bond Formation Reaction. *Comput. Theor. Chem.* **2019**, *1151*, 91–98.
- (34) Sagan, F.; Mitoraj, M. P. Kinetic and Potential Energy Contributions to a Chemical Bond from the Charge and Energy Decomposition Scheme of Extended Transition State Natural Orbitals for Chemical Valence. *J. Phys. Chem. A* **2019**, *123*, 4616–4622.
- (35) Ordon, P.; Komorowski, L. Nuclear Reactivity and Nuclear Stiffness in Density Functional Theory. *Chem. Phys. Lett.* **1998**, *292*, 22–27.
- (36) Ordon, P.; Komorowski, L. DFT Energy Derivatives and Their Renormalization in Molecular Vibrations. *Int. J. Quantum Chem.* **2005**, *101*, 703–713.
- (37) Komorowski, L.; Ordon, P. Anharmonicity of a Molecular Oscillator. *Int. J. Quantum Chem.* **2004**, *99*, 153–160.
- (38) Cohen, M. H.; Ganduglia-Pirovano, M. V.; Kudrnovsky, J. Electronic and Nuclear Chemical Reactivity. *J. Chem. Phys.* **1994**, *101*, 8988–8997.
- (39) Ayers, P. W.; Anderson, J. S. N.; Bartolotti, L. J. Perturbative Perspectives on the Chemical Reaction Prediction Problem. *Int. J. Quantum Chem.* **2005**, *101*, 520–534.
- (40) Gazquez, J. L. Perspectives on the Density Functional Theory of Chemical Reactivity. *J. Mex. Chem. Soc.* **2008**, *52*, 3–10.
- (41) Liu, Shu-B. Conceptual Density Functional Theory and Some Recent Developments. *Acta Phys.-Chim. Sin.* **2009**, *25*, 590–600.
- (42) Cardenas, C.; Echegaray, E.; Chakraborty, D.; Anderson, J. S. M.; Ayers, P. W. Relationships Between the Third-order Reactivity Indicators in Chemical Density Functional Theory. *J. Chem. Phys.* **2009**, *130*, 244105.
- (43) Komorowski, L.; Ordon, P. Vibrational Softening of Diatomic Molecules. *Theor. Chem. Acc.* **2001**, *105*, 338–344.
- (44) Sobolewski, A. Ab Initio Study of the Potential Energy Functions Hydrogen Transfer in Formamide, its Dimer and its Complex with Water. *J. Photochem. Photobiol., A* **1995**, *89*, 89–97.
- (45) Gresh, N.; Guo, H.; Salahub, D. R.; Roques, B. P.; Kafafi, S. A. Critical Role of Anisotropy for the Dimerization Energies of Two Protein-Protein Recognition Motifs: cis-N-Methylacetamide versus a beta-Sheet Conformer of Alanine Dipeptide. A Joint ab Initio, Density Functional Theory, and Molecular Mechanics Investigation. *J. Am. Chem. Soc.* **1999**, *121*, 7885–7894.
- (46) Hroudá, V.; Florián, J.; Polášek, M.; Hobza, P. Double Proton Transfer: From the Formamide Dimer to the Adenine–Thymine Base Pair. *J. Phys. Chem.* **1994**, *98*, 4742–4747.
- (47) Gould, I. R.; Hillier, I. H. Accurate Calculations of the Oxo-Hydroxy Tautomers of Uracil. *J. Chem. Soc., Perkin Trans. 2* **1990**, 329–330.
- (48) Wang, X.-C.; Nichols, J.; Feyereisen, M.; Gutowski, M.; Boatz, J.; Haymet, A. D. J.; Simons, J. Ab Initio Quantum Chemistry Study of Formamide-Formamidic Acid Tautomerization. *J. Phys. Chem.* **1991**, *95*, 10419–10424.

- (49) Langley, C. H.; Allinger, N. L. Molecular Mechanics (MM4) and ab Initio Study of Amide-Amide and Amide-Water Dimers. *J. Phys. Chem. A* **2003**, *107*, 5208–5216.
- (50) Hobza, P.; Havlas, Z. Counterpoise-corrected Potential Energy Surfaces of Simple H-bonded Systems. *Theor. Chem. Acc.* **1998**, *99*, 372–377.
- (51) Florián, J.; Johnson, B. G. Structure, Energetics, and Force Fields of the Cyclic Formamide Dimer: MP2, Hartree-Fock, and Density Functional Study. *J. Phys. Chem.* **1995**, *99*, 5899–5908.
- (52) Neuheuser, T.; Bernd, A.; Hess, B. A. Ab Initio Calculations of Supramolecular Recognition Modes. Cyclic versus Noncyclic Hydrogen Bonding in the Formic Acid/Formamide System. *J. Phys. Chem.* **1994**, *98*, 6459–6467.
- (53) Kim, Ya.; Lim, S.; Kim, H.-J.; Kim, Yo Theoretical Study of the Double Proton Transfer in Hydrogen-Bonded Complexes in the Gas Phase and in Solution: Prototropic Tautomerization of Formamide. *J. Phys. Chem. A* **1999**, *103*, 617–624.
- (54) Fu, Ai-ping; Li, Hong-liang; Du, Dong-mei; Zhou, Zheng-yu Theoretical Study on the Reaction Mechanism of Proton Transfer in Formamide. *Chem. Phys. Lett.* **2003**, *382*, 332–337.
- (55) Podolyan, Y.; Gorb, L.; Leszczynski, J. Double-Proton Transfer in the Formamidine-Formamide Dimer. Post-Hartree-Fock Gas-Phase and Aqueous Solution Study. *J. Phys. Chem. A* **2002**, *106*, 12103–12109.
- (56) Grabowski, S. J.; Sokalski, W. A.; Leszczynski, J. The Possible Covalent Nature of N-H...O Hydrogen Bonds in Formamide Dimer and Related Systems: An Ab Initio Study. *J. Phys. Chem. A* **2006**, *110*, 4772–4779.
- (57) Vargas, R.; Garza, J.; Friesner, R. A.; Stern, H.; Hay, B. P.; Dixon, D. A. Strength of the N-H...O = C and C-H...O = C Bonds in Formamide and N-Methylacetamide Dimers. *J. Phys. Chem. A* **2001**, *105*, 4963–4968.
- (58) Brdarski, S.; Astrand, P.-O.; Karlström, G. The Inclusion of Electron Correlation in Intermolecular Potentials: Applications to the Formamide Dimer and Liquid Formamide. *Theor. Chem. Acc.* **2000**, *105*, 7–14.
- (59) Šponer, J.; Hobza, P. Interaction Energies of Hydrogen-Bonded Formamide Dimer, Formamidine Dimer, and Selected DNA Base Pairs Obtained with Large Basis Sets of Atomic Orbital. *J. Phys. Chem. A* **2000**, *104*, 4592–4597.
- (60) Talaga, P.; Brela, M. Z.; Michalak, A. ETS-NOCV Decomposition of the Reaction Force for Double-proton Transfer in Formamide-derived Systems. *J. Mol. Model.* **2018**, *24*, 27.
- (61) Wang, Y.-S.; Shen, K.-L.; Chao, S. D. A Density Functional Theory Study of Double Proton Transfer Reactions in Formamide, Formamide-Formic Acid and Formic Acid Dimers. *Chin. J. Phys.* **2017**, *55*, 719–728.
- (62) Hargis, J. C.; Vöhringer-Martinez, E.; Woodcock, H. L.; Toro-Labbé, A.; Schafer, H. F., III. Characterizing the Mechanism of the Double Proton Transfer in the Formamide Dimer. *J. Phys. Chem. A* **2011**, *115*, 2650–2657.
- (63) Inostroza-Rivera, R.; Herrera, B.; Toro-Labbé, A. Using the Reaction Force and the Reaction Electronic Flux on the Proton Transfer of Formamide Derived Systems. *Phys. Chem. Chem. Phys.* **2014**, *16*, 14489–14495.
- (64) Smaga, A.; Sadlej, J. Computational Study on Interaction Energy Changes During Double Proton Transfer Process. *Comput. Theor. Chem.* **2012**, *998*, 120–128.
- (65) Beg, Hasibul; Sankar, Prasad De; Ash, Sankarlal; Misra, Ajay Use of Polarizability and Chemical Hardness to Locate the Transition State and the Potential Energy Curve for Double Proton Transfer Reaction: A DFT Based Study. *Comput. Theor. Chem.* **2012**, *984*, 13–18.
- (66) Wang, W.; Cao, G. Investigations of Double Proton Transfer and One-electron Oxidation Behavior in Double H-bonded Glycine-Formamide Complex in the Gas Phase. *J. Mol. Struct.: THEOCHEM* **2005**, *726*, 17–24.
- (67) Beegum, S.; Mary, Y. S.; Varghese, H. T.; Panicker, C. Y.; Armaković, S.; Armaković, S. J.; Zitko, J.; Dolezal, M.; Van Alsenoye, C. Vibrational Spectroscopic Analysis of Cyanopyrazine-2-carboxamide Derivatives and Investigation of Their Reactive Properties by DFT Calculations and Molecular Dynamics Simulations. *J. Mol. Struct.* **2017**, *1131*, 1–15.
- (68) Pejov, L.; Panda, M. K.; Moriwaki, T.; Naumov, P. Probing Structural Perturbation in a Bent Molecular Crystal with Synchrotron Infrared Microspectroscopy and Periodic Density Functional Theory Calculations. *J. Am. Chem. Soc.* **2017**, *139*, 2318–2328.
- (69) Dominikowska, J.; Jabłoński, M.; Palusiak, M. Feynman Force Components: Basis for a Solution to the Covalent vs. Ionic Dilemma. *Phys. Chem. Chem. Phys.* **2016**, *18*, 25022–25026.
- (70) Zaklika, J.; Komorowski, L.; Ordon, P. The Bond Fragility Spectra for the Double Proton Transfer Reaction, in the Formic Acid Type Dimers. *J. Phys. Chem. A* **2019**, *123*, 4274–4283.
- (71) Zaklika, J.; Komorowski, L.; Ordon, P. Evolution of the Atomic Valence Observed by the Reaction Fragility Spectra on the Reaction Path. *J. Mol. Model.* **2019**, *25*, 134.
- (72) Echegaray, E.; Toro-Labbé, A. Reaction Electronic Flux: A New Concept To Get Insights into Reaction Mechanisms. Study of Model Symmetric Nucleophilic Substitutions. *J. Phys. Chem. A* **2008**, *112*, 11801–11807.
- (73) Martínez-Araya, J. I.; Toro-Labbé, A. Reaction Electronic Flux as a Fluctuation of Relative Interatomic Electronic Populations. *J. Phys. Chem. C* **2015**, *119*, 3040–3049.
- (74) Frisch, M. J.; Trucks, G. W.; Schlegel, H. B.; Scuseria, G. E.; Robb, M. A.; Cheeseman, J. R.; Scalmani, G.; Barone, V.; Petersson, G. A.; Nakatsuji, H.; et al. *Gaussian 09*, Revision A.02; Gaussian, Inc.: Wallingford, CT, 2009.
- (75) Mayer, I. Bond Order and Valence Indices. *J. Comput. Chem.* **2007**, *28*, 204–221.
- (76) Toro-Labbé, A. Characterization of Chemical Reactions from the Profile of Energy, Chemical Potential, and Hardness. *J. Phys. Chem. A* **1999**, *103*, 4398–4403.
- (77) Luty, T.; Ordon, P.; Eckhardt, C. J. A model for mechanochemical transformations: Applications to molecular hardness, instabilities, and shock initiation of reaction. *J. Chem. Phys.* **2002**, *117*, 1775–1785.
- (78) Politzer, P.; Murray, J. S. A Look at Bonds and Bonding. *Struct. Chem.* **2019**, *30*, 1153–1157.